Journal of Engineering Research

Volume 7
Issue 5 *This is a Special Issue from the Applied Innovative Research in Engineering Grand Challenges (AIRGEC) Conference, (AIRGEC 2023), Faculty of Engineering, Horus University, New Damietta, Egypt, 25-26 October 2023*

Article 1

2023

# Design and Implementation of a 2.4 GHz Millimeter Wave Radar System for Soil Water Content Detection

Amr Hussein, Ahmed M. Elkhawaga, hossam Mohamed kasem, Mohamed Dabaon

Engineering Research (ERJ)
Vol. 7 – No. 5, 2023

ISSN: 2356-9441 https://erjeng.journals.ekb.eg/ e ISSN: 2735-4873

# Design and Implementation of a 2.4 GHz Millimeter Wave Radar System for Soil Water Content Detection

**Amr H. Hussein[3,4], Ahmed M. Elkhawaga[3], Hossam M. Kassem[3,4], and Mohamed A. Dabaon[1,2]**

[1] Civil Engineering Dept., Faculty of Engineering, Tanta University, Tanta, Egypt.

[2] Civil Engineering Dept., Faculty of Engineering, Horus University Egypt (HUE), New Damietta, Egypt

Email :mdabaon@horus.edu.eg

[3] Electronics and Electrical Communications Engineering Dept., Faculty of Engineering, Tanta University, Tanta, Egypt.

Email: amr.abdallah@f-eng.tanta.edu.eg, amrvips@yahoo.com, Hossam.kasem@f-eng.tanta.edu.eg

[4] Electronics and Electrical Communications Engineering Dept., Faculty of Engineering, Horus University Egypt, New Damietta, Egypt.

Email: ahussein@horus.edu.eg , hkasem@horus.edu.eg

***Abstract*- Because water has the highest real permittivity value, close to 80, compared to dry soils' real permittivity, which ranges from 3 to 15, measuring a soil's permittivity is strongly reliant on its moisture content. Furthermore, increased relative permittivity leads to a larger reflectivity coefficient. According to these perspectives, adding water to dry soil generates notable changes in wet soil permittivity and modifies the reflectance and characteristics of incident electromagnetic waves (EMWs) at the soil-air interface. Thus, the soil water content (SWC) may be reliably determined by recording variations in the properties of incident EMWs compared to a reference dry soil case. This inspired us to develop a millimeter wave radar system to measure the SWC. In this paper, the design and hardware implementation of a 2.4 GHz millimeter wave radar system is introduced for SWC measurement. The SWC measurement principle of the proposed system is based on measuring the reflection coefficient of the soil-air interface. The received analog signal is amplified before it is converted into a digital signal that is sent by the Arduino microcontroller to the computer buffer via the serial communication port to be analyzed using the designed MATLAB codes.**

***Keywords*- Electromagnetic wave, Frequency modulated continuous wave (FMCW), Single frequency continuous wave (SFCW), Radar system, Soil water content (SWC), Wideband antenna (WBA).**

## I. INTRODUCTION

Since dry soils' actual permittivity ranges from 3 to 15, and water's real permittivity is close to 80, measuring a soil's permittivity is highly dependent on its moisture content [1]. Because rainfall is regarded as the primary cause of landslides, the influence of rainfall on the growth of soil water content and its flow plays an important role in slope instability [2– 3]. Some of the precipitation that falls on the slope surface infiltrates into the soil, while the rest flows as surface groundwater. When water infiltrates the slope, the suction matric diminishes as soil moisture increases, causing the soil structure to shift and reducing friction and cohesive forces between particles [4]. As a result, the negative pressure of pore water between soil particles reduces, and shift power decreases, affecting slope stability [5–7]. For soil water content, the Hygrometer sensor YL-69 is used in [8]. This sensor is made up of two electrodes and measures electrical resistance. This soil humidity sensor measures the humidity content of the surrounding environment. The current is sent to the electrode via the soil, and the resistance to the current within the soil indicates soil humidity.

In [9], the manufacture of a low-leakage-current type impedance sensor chip employing shield structures has been introduced. When compared to other semiconductor-type sensors, the low-limit detection of soil-water-content measurement was enhanced. Shield structures were created beneath the impedance sensor region. In addition, a new operational circuit is developed to separate the leakage current in order to measure the weak signal current and eliminate the leakage current. The sensor was capable of detecting low water content of 10% or less. In [10], the impact of soil salinity and volumetric water content on the relationship between soil moisture and dielectric permittivity has been studied. The soil complex dielectric permittivity depends mainly on soil volumetric water content and salinity, but other soil properties such as temperature, density, and clay content can also significantly impact its dielectric properties. This impact significantly affects the electromagnetic wave propagation, scattering, and reflection from soil-air interface. The scattering feature of soil moisture has become an important topic of research in recent decades, with substantial implications for the global water cycle, energy balance, and weather climatic changes. One of the prerequisites for solving the global water cycle pattern, hydrological model, crop growth monitoring, and drought monitoring is the monitoring of soil water content on a regional and worldwide scale. Many experiments have previously been conducted to study the sensitivity of microwave sensors to soil water content, and various synthetic aperture radar (SAR) photographs have broadened scientific research on microwave use [11]. The open-ended probe with an antenna (OE-A) was presented in [12] as an adequate instrument for measuring soil water content. Two types of mineral soils with varying moisture

Doi: 10.21608/ERJENG.2023.237513.1254

levels were evaluated using a vector network analyzer (VNA) in the frequency range from 1 MHz to 6 GHz.

In this paper, a new design and hardware implementation of a multifunction millimeter wave radar system is introduced. The proposed radar operates in the frequency range of 1.3 GHz to 2.7 GHz and can be programmed and readjusted to perform a variety of functions such as spectrum analyzer to measure the impulse response of radio frequency identification (RFID) tags indicating their scattering parameters S_21 or S_12, detection of non-metallic objects such as human bodies, detection of metallic objects, detection of cracks in concrete, and detection of soil water content, which is the primary target of the paper. The proposed radar system that is mainly based on the utilization of an 8 GHz radio frequency (RF) power detector that can detect signals of frequencies from 10 MHz to 8000 MHz. It gives the proposed radar the ability to detect a wide variety of objects with different resolutions. Furthermore, it has the ability to work over wide range of frequencies, which indeed enables the system to measure different liquids content in a soil.

## II. Proposed Millimeter Wave Radar System

Traditionally, the water content in soil is expressed gravimetrically or volumetrically. The mass of water per mass of dry soil is referred to as gravimetric water content. It is measured by first weighing a wet soil sample in an oven, then drying the sample to remove the water and weighing the dried soil. The gravimetric water content, on the other hand, is time-consuming, destructive, and only provides a snapshot at a time. It is occasionally necessary to give a time series of measurements for profile sensing across time while avoiding destructive sampling. In this paper, the design and hardware implementation of a 2.4 GHz millimeter wave radar system is introduced for soil water content measurement. A radar system is a remote sensing device that offers a time series and powerful spatial sampling. The soil water content measurement principle of the proposed system is based on measuring the reflection coefficient of the soil-air interface.

Figure 1 shows the block diagram of the proposed radar system that is mainly based on the utilization of an 8000 MHz radio frequency (RF) power detector that can detect signals of frequencies from 10 MHz to 8000 MHz. It gives the proposed radar the ability to detect a wide variety of objects with different resolutions. The proposed radar system is marked by simplicity, flexibility, and cheapness. It can be programmed to perform multifunction such as detecting concrete cracks, metal bars, hidden objects, and soil water content. The radar has two operating modes either generating a single frequency continuous wave (SFCW) signal or a frequency modulated continuous wave (FMCW) signal using an RF voltage-controlled oscillator (VCO). The reflected RF signal from the object or soil under test is received at the receive antenna and converted into analog voltage by the RF power detector. The analog voltage signal is then amplified before it is converted into a digital signal that is sent by the Arduino microcontroller to the computer buffer via the serial communication port to be analyzed using the designed MATLAB codes according to the required application and the criteria of measurement. In other words, the radar scanning technique and detection algorithm will be selected and performed on the received signal from the object according to the desired function.

The basic building blocks and components of the proposed radar system are described below. The basic building blocks can be divided into five main blocks as follows:

1. Radar transmitter.
2. Radar receiver.
3. Control unit and monitoring system.
4. Radar TX/RX Antennas.
5. Sawtooth and DC signal generators.

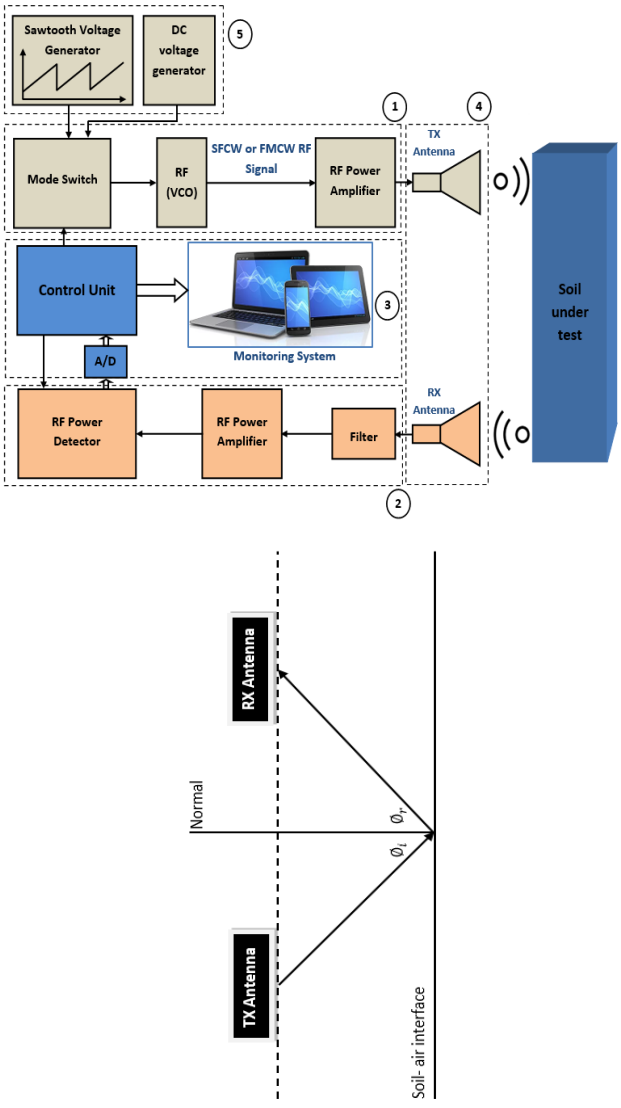


**Fig. 1.** Block diagram of the proposed millimeter wave radar system for soil water content detection.

**a) Radar Transmitter**

The transmitter consists of four elements i.e., the sawtooth voltage generator, RF voltage-controlled oscillator (VCO),

Journal of Engineering Research (ERJ)
Vol. 7 – No. 3, 2023
©Tanta University, Faculty of Engineering
ISSN: 2356-9441 https://erjeng.journals.ekb.eg/ e ISSN: 2735-4873

RF power amplifier, and the transmit antenna. The main idea of the transmitter is based on generating a single frequency continuous wave signal or a constant amplitude 1300 MHz to 2700 MHz frequency modulated continuous wave (FMCW) that are amplified before they are fed to the TX antenna. When the radiated RF signal falls on a target, the FMCW amplitude will be modulated before it is reflected back to the RX antenna. The basic building block of the radar transmitter is the (ZX95-2700A+) VCO. It provides RF signal with output power 3.3 dBm and tuning voltage from 0.15 V to 25 V. Thereby, for 1300-2700 MHz FMCW generation, the VCO is supplied by a periodic sawtooth signal of frequency $f = 1KHz$ and period $T = 1msec$, minimum amplitude $V_{min} = 0.15V$, and maximum amplitude $V_{max} = 25V$. The corresponding FMCW signal will be repeated every period T. The generated FMCW signal is amplified by the (ZJL-5G) fixed gain power amplifier. The amplifier operating frequency range is from 20 MHz to 5 GHz. The amplifier's maximum gain is 9dB with maximum output power of 9.5 dBm. Finally, the amplified FMCW signal is fed to the transmit antenna through a 50Ω coaxial cable. For single frequency operation, the mode switch is set to select the DC voltage generator. In this case, the RF VCO generates a SFCW RF signal.

**b) Radar Receiver**

At the receiving side, the received RF signal at the receive antenna is passed through a low pass filter (LPF) to remove the noise and unwanted high frequency components. The utilized LPF is the (SLP-2950+A) LPF with passband from DC to 2700MHz and maximum stopband attenuation of 40dB. The filtered signal is then amplified by the (ZJL-5G) fixed gain power amplifier and fed to the RF power detector. The utilized RF power detector is the (ZX47- 60LN+) detector that converts the received RF signal into DC voltage. The power detector has an input power dynamic range from -60 dBm to +5 dBm over operating frequency range from 10 MHz to 8 GHz. Generally, the RF power detector detects the RF signal power and generates a DC voltage signal whose amplitude is proportional to the received signal power.

**c) Control Unit and Monitoring System**

The main unit or the main brain of the radar system is Arduino Uno. Arduino board is based on the ATMEGA328 which has all features of microcontrollers. It is simply connected to the computer using a USB cable which provides the required power to start the device operation and a mean for data transfer. The ATMEL16U2 is easily programmed using the USB cable and there is no need for a separate burner. The Arduino supplies the control voltages simultaneously to the sawtooth signal generator and the RF power detector for synchronized operation. The analog output signal from the RF power detector is converted into a digital signal using analog to digital converter (A/D) and fed to the microcontroller, which transfers it to the monitoring unit.

**d) TX/RX Wideband Antenna Element**

The development of wireless technologies like an ultra-wideband antenna technology, have increased demand for wideband (WB) antennas. In these systems, printed wide slot antennas have received much attention owing to their wideband matching characteristics and omnidirectional radiation patterns. In this section, a design of a wideband antenna with microstrip line feed is presented. The total bandwidth of the antenna is controlled by optimizing the width D and the length H of the fork-shaped tuning stub. Fig. 2 shows the geometry and dimensions of the proposed slot antenna with a (R=19 mm) radius semi-circle-like aperture. The circle radius is at the center of the substrate. The antenna is designed using the CST microwave studio software package on an FR4 (lossy) substrate with ε_r=4.5 and h=1.5 mm.

Fig. 3 compares the scattering parameter of the antenna element produced using CST software to the experimental measurements of the manufactured antenna element acquired using the VNA (HP8719Es). The simulation results show that the developed antenna element has a broad frequency range from 1.86 to 4.43 GHz. The results show that the manufactured antenna element has a broad frequency range from 2.1 GHz to more than 6 GHz [13].

Fig. 4 (a), (b), and (c) show the simulated far field radiation pattern of the antenna element at the frequency f=2.4 GHz. The antenna gives a nearly omnidirectional radiation pattern in the H-plane and a dipole-like radiation pattern in the E-plane as shown in Fig. 4-b and Fig. 4-c, respectively.

**e) Sawtooth Signal Generator**

In this section, the circuit diagrams of a sawtooth signal generator and the required power supplies are introduced. The sawtooth signal generator is used to feed the RF VCO to generate a frequency modulated continuous wave signal (FMCWS). The basic building block of the radar transmitter is the (ZX95-2700A+) VCO. It provides RF signal with output power 3.3 dBm and tuning voltage from 0.15 V to 25 V. Thereby, for 1300-2700 MHz FMCW generation, the VCO is supplied by a periodic sawtooth signal of frequency $f = 1KHz$ and period $T = 1msec$, minimum amplitude $V_{min} = 0.15V$, and maximum amplitude $V_{max} = 25V$ as shown in Fig. 5. The corresponding FMCW signal will be repeated every period T as shown in Fig. 6.

Doi: 10.21608/ERJENG.2023.237513.1254

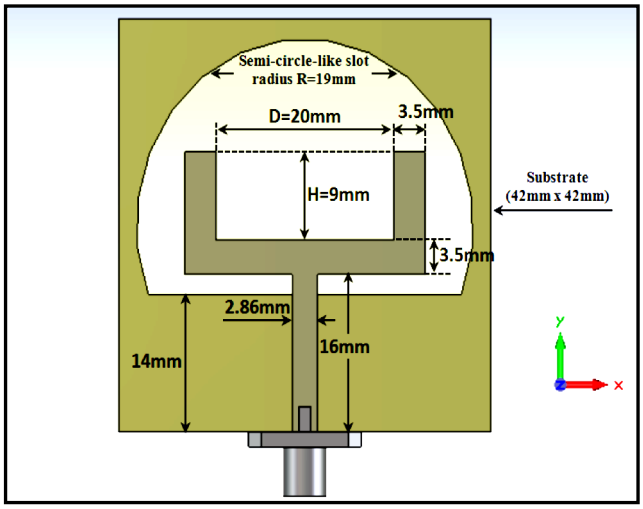


**Fig. 2.** Configuration of the semi-circle-like slot antenna designed using the CST software using FR4 (lossy) substrate with $\varepsilon_r = 4.5$ and $h = 1.5\ mm$ [13].

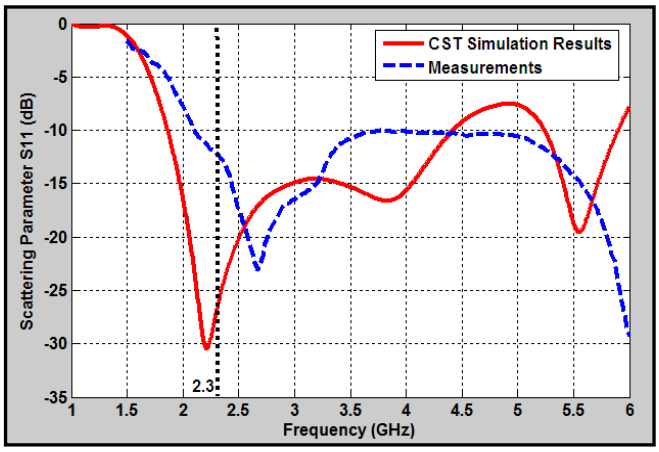


**Fig. 3.** The scattering parameter $S_{11}$ of the semi-circle-like slot antenna element using the CST simulation compared to the experimental measurements [13].

## III. Hardware Implementation of the Proposed Radar System

In this section, the hardware implementation of the proposed radar system is introduced. Fig. 7 shows the assembly of the entire radar system. In this work, the single frequency

continuous wave (SFCW) signal mode of operation is used to detect the soil water content at a single frequency f=2.4 GHz.

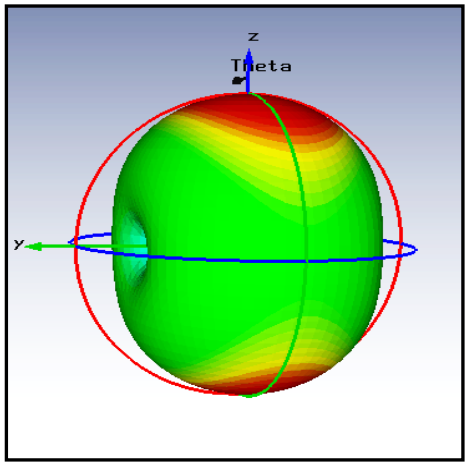


(a)

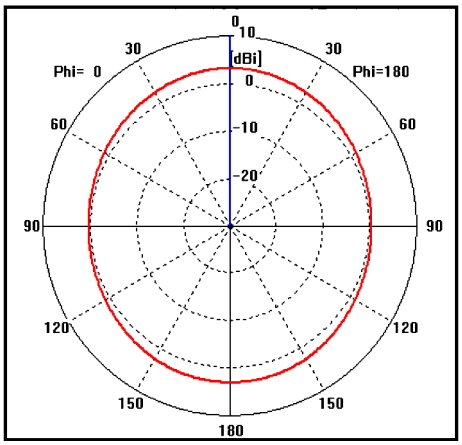


(b)

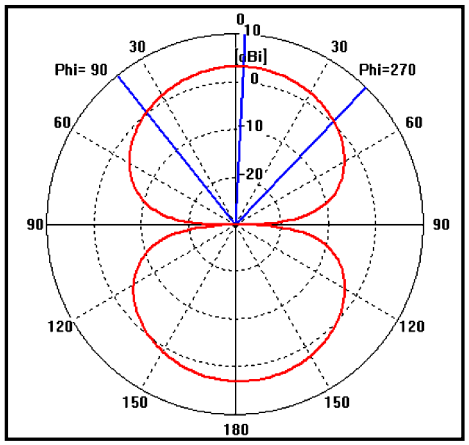


(c)

**Fig. 4.** The simulated radiation pattern of the proposed antenna element at the power divider resonance frequency 2.4 GHz (a) 3D plot of the pattern, (b) Polar plot of the pattern in the H-plane, and (c) Polar plot of the pattern in the E- plane [13].

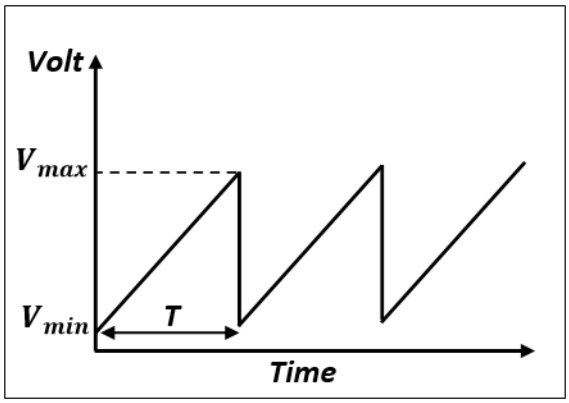


**Fig. 5.** The periodic sawtooth signal of period $T = 1msec$, minimum amplitude $V_{min} = 0.15V$, and maximum amplitude $V_{max} = 25V$.

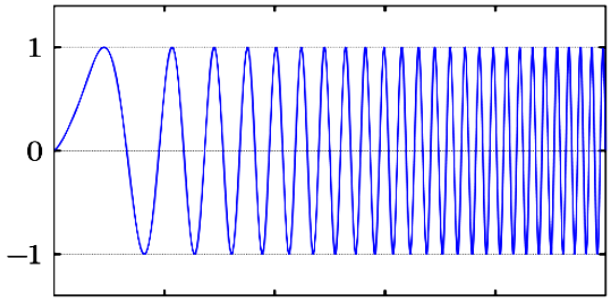


**Fig. 6.** The FMCW signal that is repeated every period $T$ of the designed sawtooth signal.

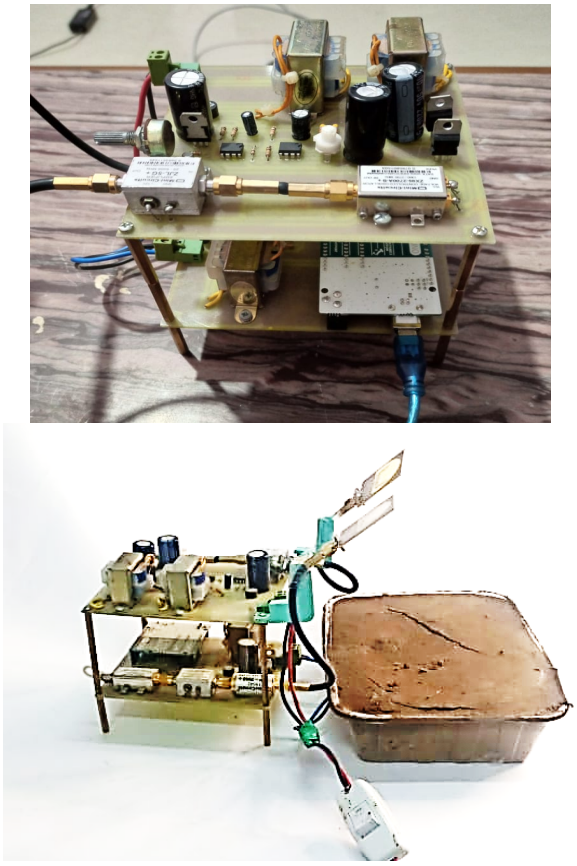

**Fig. 7.** Hardware implementation of the entire radar system (a) front view and (b) side view.

## V. The Soil Water Content Measurement Principle

The proposed millimeter wave radar system's soil water content measurement technique relies on determining the reflection coefficient Γ of the soil-air interface, which is related to the soil permittivity $\varepsilon_s$ by [14]:

$$\Gamma = \left(1 - \sqrt{\varepsilon_s}\right)/\left(1 + \sqrt{\varepsilon_s}\right) \quad (1)$$

This equation can be reformulated to express $\varepsilon_{soil}$ in terms of $\Gamma$ as follows:

$$\varepsilon_s = ((1 - \Gamma)/(1 + \Gamma))^2 \quad (2)$$

The transmit and receive antennas are spaced $h$ apart from the soil-air interface and configured such that the incidence angle $\emptyset_i$ and the reflection angle $\emptyset_r$ of the electromagnetic wave are equal as illustrated in Fig. 1, which represents common mid-point reflection mode. The receiving antenna detects the reflected wave at the soil-air interface with a measured amplitude $A_r$. The reflection coefficient is defined as the ratio of the measured amplitude $A_r$ to the ideal reflection amplitude $A_m$ and can be expressed as:

$$\Gamma = A_r/A_m \quad (3)$$

whereas the ideal reflector may be thought of as a metal plate bigger than the radar antenna's footprint. The radar's footprint may be approximated by the diameter of the antenna's first Fresnel zone F, which is given by [14]:

$$F = \sqrt{\left(\frac{\lambda}{4} + 2h\lambda\right)} \quad (4)$$

where λ=c/f is the free space wavelength, c is the speed of light that equals c=3×10^8 m/sec, f is the operating frequency, and $h$ is the height of the antenna from the soil-air interface. Substituting (3) in (2), the soil permittivity $\varepsilon_s$ can be expressed as:

$$\varepsilon_s = \left((1 - \frac{A_r}{A_m})/(1 + \frac{A_r}{A_m})\right)^2 \quad (5)$$

The empirical Topp's equation, which is stated below, may be used to compute the volumetric soil water content, $\theta_v\ (m^3\ m^{-3})$, from soil permittivity $\varepsilon_s$.

$$\theta_v = -5.3 \times 10^{-2} + 2.92 \times 10^{-2} \times \varepsilon_s - 5.5 \times 10^{-4} \times {\varepsilon_s}^2 + 4.3 \times 10^{-6} \times {\varepsilon_s}^3 \quad (6)$$

After measuring $A_r$ with the RF power detector, $\varepsilon_s$ is computed directly from (5) and the equivalent volumetric soil water content, $\theta_v\ (m^3\ m^{-3})$, is determined from (6).

## VI. Experimental Measurements of Soil Water Content Using the Proposed Radar System

This section introduces the experimental measurement of soil water content using the proposed millimeter wave radar system. The experimental setup of the system is the initial stage of the measurement procedure. In this stage, the radar operating frequency is set to $f = 2.4\ GHz$.

Doi: 10.21608/ERJENG.2023.237513.1254

Accordingly, the operating wavelength is $\lambda = c/f = 0.125\ m$. The antenna spacing from the soil-air interface is set to $h = 0.5\ m$. The calculated Fresnel zone F equals 0.3953 m that represents the diameter of the ideal reflecting plate required to determine amplitude of the wave at perfect reflection is $A_m$. The data collecting and measurement stage comes next. In this stage, the ideal reflector is chosen as a circular metal disc with a diameter of $d = 0.3953\ m$ that results in a measured amplitude of $A_m$ =0.25 V. Following $A_m$ measurement, the ideal reflector plate is removed and replaced with a 2.25 liters dry soil sample placed in a plastic container of dimensions $(15 \times 15 \times 15)\ cm^3$.

Water is gradually added to the dry soil sample in modest increments of $\Delta = 0.025\ liter$. The amplitude of the reflected wave $A_r$ is measured at each step, and the associated reflection coefficient Γ is computed according to (3), as listed in Table 1. The estimated reflection coefficient versus the added soil water content is shown in Fig. 8. It is clear that as the water content increases, the reflection coefficient increases.

**Table 1.** Volumetric water content $(\theta_v)$, measured reflected wave amplitude $A_r$, and estimated reflection coefficient Γ at $A_m = 0.25\ V$.

| Step number | Volumetric water content $(\theta_v)$ | Measured $A_r$ in volts | Reflection coefficient (Γ) |
|---|---|---|---|
| 1 | 0 | 0.0263 | 0.1050 |
| 2 | 0.025 | 0.0292 | 0.1169 |
| 3 | 0.050 | 0.0320 | 0.1281 |
| 4 | 0.075 | 0.0337 | 0.1346 |
| 5 | 0.100 | 0.0350 | 0.1400 |
| 6 | 0.125 | 0.0350 | 0.1400 |
| 7 | 0.150 | 0.0364 | 0.1455 |
| 8 | 0.175 | 0.0367 | 0.1469 |
| 9 | 0.200 | 0.0389 | 0.1555 |
| 10 | 0.225 | 0.0391 | 0.1563 |
| 11 | 0.250 | 0.0407 | 0.1627 |
| 12 | 0.275 | 0.0411 | 0.1642 |
| 13 | 0.300 | 0.0417 | 0.1667 |
| 14 | 0.325 | 0.0421 | 0.1683 |
| 15 | 0.350 | 0.0451 | 0.1804 |
| 16 | 0.375 | 0.0482 | 0.1927 |
| 17 | 0.400 | 0.0496 | 0.1983 |
| 18 | 0.425 | 0.0498 | 0.1990 |
| 19 | 0.450 | 0.0502 | 0.2009 |
| 20 | 0.475 | 0.0506 | 0.2024 |
| 21 | 0.5 | 0.0510 | 0.2040 |

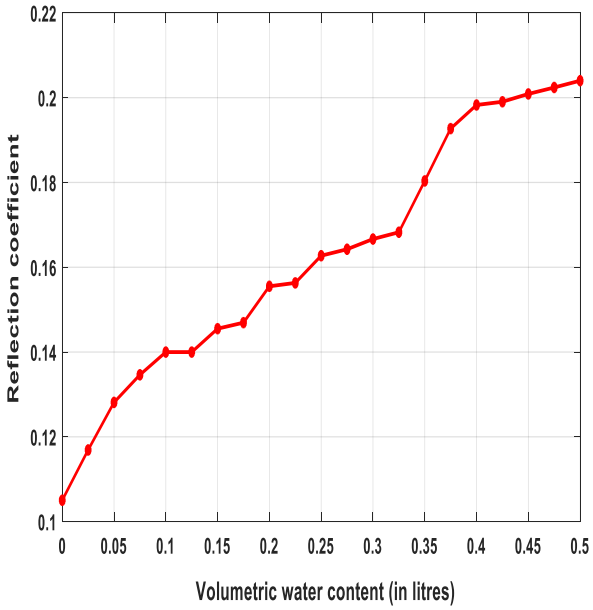


Fig. 8. The estimated reflection coefficient versus soil water content.

## VII. Conclusion

The hardware implementation of a proposed 2.4 GHz millimeter wave system for soil water content measurements is presented in this paper. The proposed system is distinguished by its simplicity, adaptability, and low cost. The suggested system's soil water content measurement principle is based on measuring the reflection coefficient of the soil-air interface. This is due to the fact that adding water to dry soil causes significant changes in wet soil permittivity as well as changes in the reflectance and properties of incident electromagnetic waves at the soil-air interface. It has been observed that as the water content increases, so does the reflection coefficient.

## Acknowledgment

The authors gratefully acknowledge Horus University, Egypt, New Damietta, Egypt for its support in this research.

**Funding:** This work was not supported by any Foundation.

**Conflicts of Interest:** The authors declare no competing interests.

## References

[1] Mohamed, A.-M.O., Paleologos, E.K. Chapter 16—Dielectric Permittivity and Moisture Content. In Fundamentals of Geoenvironmental Engineering; Mohamed, A.-M.O., Paleologos, E.K., Eds.; Butterworth-Heinemann: Oxford, UK, 2018; pp. 581–637.

Journal of Engineering Research (ERJ)
Vol. 7 – No. 3, 2023
©Tanta University, Faculty of Engineering
ISSN: 2356-9441 https://erjeng.journals.ekb.eg/ e ISSN: 2735-4873

[2] M. Mukhlisin and M.R. Taha, "Numerical Model of Antecedent Rainfall Effect on Slope Stability at a Hillslope of Weathered Granitic Soil Formation. Journal Geological Society of India", vol. 79, pp. 525- 531, 2012. [Scopus, ISI, Q4, IF: 0.567, ISSN No: 0016-7622.

[3] M. Mukhlisin, S.J. Matlan, M.J. Ahlan, and M.R. Taha, "Analysis of Rainfall Effect to Slope Stability in Ulu Klang, Malaysia. Jurnal Teknologi (Science and Engineering)", vol. 72:3, pp. 15–21, 2015.

[4] G. Nurly, M.L. Lee, and M. Asof, "Transient seepage and slope stability analysis for rainfall-induced landslide: A case study". Malaysian Journal of Civil Engineering vol. 18(1), pp. 1-13, 2006.

[5] J. M. Gasmo, H. Rahardjo, and E.C. Leong, "Infiltration Effects on Stability of a Residual Soil Slope, Computers And Geotechnics", vol. 26, pp. 145-165, 2000.

[6] BK. Bujang, F. H. Ali, and T.H. Low, "Water Infiltration Characteristics of Unsaturated Soil Slope and its Effect on Suction and Stability, Geotechnical and Geological Engineering", vol. 24, pp. 1293- 1306, 2006.

[7] M. Mukhlisin, M.R. Baidillah, M.R. Taha, and A. ElShafie, "Effect of Soil Water Retention Model on Slope Stability Analysis. International Journal of the Physical Sciences", vol. 6, no. 19, pp. 4629 – 4635, 2011.

[8] A. Suharjono, M. Mukhlisin and N. K. M. Alfisyahrin, "The development of soil water content detector," 2017 4th International Conference on Information Technology, Computer, and Electrical Engineering (ICITACEE), pp. 154-157, 2017.

[9] M. Futagawa et al., "Fabrication of a low leakage current type impedance sensor to monitor soil water content for slope failure prognostics," 2017 19th International Conference on Solid-State Sensors, Actuators and Microsystems (TRANSDUCERS), pp. 1136-1139, 2017.

[10] A. Szypłowska, J. Szerement, A. Lewandowski, M. Kafarski, A. Wilczek and W. Skierucha, "Impact of Soil Salinity on the Relation Between Soil Moisture and Dielectric Permittivity," 2018 12th International Conference on Electromagnetic Wave Interaction with Water and Moist Substances (ISEMA), pp. 1-3, 2018.

[11] L. He, Y. Li, Y. Li and H. Wu, "Sensitivity of Backscatter to Soil Water Content At L-, S-, C-, and X-Bands in SEMI-Flooded Area," IGARSS 2019 - 2019 IEEE International Geoscience and Remote Sensing Symposium, pp. 7108-7111, 2019.

[12] A. Woszczyk et al., "A Modified Open-Ended Probe as a Reliable Tool for Measurements of Soil Water Content," 2020 Baltic URSI Symposium (URSI), pp. 161-164, 2020.

[13] A. H. Hussein, M. A. Metawe'e, H. H. Abdullah," Hardware implementation of antenna array system for maximum SLL reduction", Engineering Science and Technology, an International Journal, Elsevier, vol. 20, pp. 965–972, 2017.

[14] J. A. Huisman, S. S. Hubbard, J. D. Redman, and A. P. Annan, "Measuring Soil Water Content with Ground Penetrating Radar: A Review", Vadose Zone Journal, vol. 2, pp. 476–491, 2003.

Doi: 10.21608/ERJENG.2023.237513.1254